České vysoké učení technické v Praze
Fakulta jaderná a fyzikálně inženýrská
Katedra fyzikální elektroniky

Ing. Filip Novotný

Metal particle nanostructures: synthesis and applications

Doktorský studijní program: Aplikace přírodních věd
Studijní obor: Fyzikální inženýrství

Teze disertace k získání akademického titulu „doktor“, ve zkratce „Ph.D.“

Praha, leden 2015

Disertační práce byla vypracována v kombinované formě doktorského studia na Katedře fyzikální elektroniky Fakulty jaderné a fyzikálně inženýrské ČVUT v Praze.

Uchazeč: **Ing. Filip Novotný**
Fakulta jaderná a fyzikálně inženýrská ČVUT
Břehová 7, 115 19 Praha 1
filip.novotny@fjfi.cvut.cz

Školitel: **Prof. Ing. Pavel Fiala, CSc.**
Fakulta jaderná a fyzikálně inženýrská ČVUT
Břehová 7, 115 19 Praha 1
pavel.fiala@fjfi.cvut.cz

Školitel – specialista: **RNDr. Jan Proška**
Fakulta jaderná a fyzikálně inženýrská ČVUT
Břehová 7, 115 19 Praha 1
jan.proska@fjfi.cvut.cz

Oponenti: **Prof. Ing. Eduard Hulicius, CSc.**
Fyzikální ústav AV ČR, v. v. i.
Cukrovarnická 10
162 00 Praha 6
hulicius@fzu.cz

Prof. RNDr. Jan Valenta, PhD.
Matematicko-Fyzikální fakulta UK
Ke Karlovu 3
121 16 Prague 2
jan.valenta@mff.cuni.cz

Teze byly rozeslány dne: ……………

Obhajoba dizertace se koná dne **13.02.2015** v **13:00** hodin před komisí pro obhajobu disertační práce ve studijním oboru fyzikální inženýrství v zasedací místnosti **č. 121** v budově Fakulty jaderné a fyzikálně inženýrské ČVUT v Praze, Trojanova 13, Praha 2.

S disertací je možno se seznámit v děkanátě Fakulty jaderné a fyzikálně inženýrské ČVUT v Praze, na oddělení pro vědeckou a výzkumnou činnost, Břehová 7, Praha 1.

Doc. Ing. Ladislav Pína, DrSc.
předseda komise pro obhajobu disertační práce ve studijním oboru fyzikální inženýrství
Fakulta jaderná a fyzikálně inženýrská, Břehová 7, Praha

LIST OF CONTENTS

1 INTRODUCTION AND STATE OF THE ART

The application of gold nanorods (AuNRs) has increased tremendously in the past decade [1]. Here I would like to point out two main directions. First, the unique optical response of the nanoscopic AuNR, governed by the localised surface plasmon resonance, provides it with extremely large absorption and scattering cross sections. This property of the plasmonic nanoparticles (NPs) in general, and the noble chemical properties of gold, have sparked new scientific field called theranostics. For this new scientific field are the AuNR the number one choice of advanced multifunctional workers in the sense of nanoscopic probes capable of being identified by optical methods and therapy by optical energy absorption [2]. Second, the coupling of the plasmonic NP's LSPR at close distance creates new exotic modes, which further broadens the extensive AuNR tunability in the optical and NIR region. The very basic particle dimers and trimmers are successfully used as so called "plasmon rulers", however, when the organised subunit is periodically repeated in large amount of times, exotic new optical behaviour is foretold. This novel optical "metamaterials" are the new frontier in the nanoscale material science and the utilisation of the colloidal solutions of complex shaped NPs with narrow size distributions is highly desirable approach for the technological procurement of these superstructures [3].

Finally, the combined properties of single gold NPs and their assemblies brought into existence a new scientific and technological field of theranostics [4]. Theranostics, which stands for the synergy of the words "therapy" and "diagnosis", utilizes the synergy of our ability to synthesize large population of shaped gold NPs by colloidal chemistry, the ability to cap them with biological targeting molecules, and their strong resonant optical absorption and scattering. The gold NPs will serve as modular nanosized carriers in living tissue, which can use their optothermal energy conversion for drug release or simply for the treatment by heat [5]. Or to exploit the dependence of their resonant optical properties on the change of the dielectric surroundings and/or by the close vicinity of another plasmonic NP [1].

1.1 Seeded growth method for gold nanorod synthesis

Historically, AuNRs were first prepared using electrochemical methods with porous alumina or polycarbonate template as the shape directing agents [6]. They provided the first opportunity for the researchers to experimentally study the optical properties of AuNRs. This helped to spread the recognition of the unique AuNR properties with respect to visible and near-infrared light, and in turn incite the motivation to develop the first truly wet-chemical synthesis of AuNRs, a three-stepped seeded growth approach.

Since 2005, the original seeded growth synthesis was enhanced by a number of modifications, including small organic additives to the CTAB bilayer, continuous flow synthesis, seedless approach, and gram scale versions of the mentioned syntheses. AuNRs have been also used as seeds for further overgrowing into complex anisotropic gold NPs, which possess more complex optical properties. The seeded growth method completely dominated the field of the synthesis of complex shaped gold NPs. As far as the plethora of the modifications of original seeded growth approach goes, the very fundamental questions about the principles driving the anisotropic growth are still left unanswered [7].

Figure 1.1 shows three gold colloids prepared at the author's laboratory, featuring the classical spherical nanoparticles made by Turkevich approach, but also seeded grown gold triangular nanoprisms and AuNRs. The change of the optical properites of the gold sols containing different NP shapes is apparent. In addition, from the TEM micrographs it can be clearly seen the superior shape purity of the AuNRs sample, when compared to the gold triangular nanoprisms.

Figure 1.1: An overview of the various gold sols prepared at the author's laboratory. From left to righ: gold nanopsheres, gold triangular nanoprisms, and gold nanorods. The mean volume of the particles in each solution is comparable with the others, however, the change of shape cause dramatical change in the optical properties of the colloids. The solutions contain approximately 0.05 mg of gold per millilitre. The particle concentration is in order of 10^{11} particles per millilitre. Scale bar equals 30 nm.

1.2 Applications of complex shaped metal nanoparticles

The applications of complex shaped metal nanoparticles span wide range from biomedical sensing and imaging, cancer therapy, targeted drug delivery, photonics and optoelectronics. Moreover, the anisotropic responses of complex shaped noble metal NPs provide opportunities to engineer novel optical nanomaterial as polarization filters and with clever stacking of anisotropic particles into superstructures, metamaterials exhibiting effects as plasmon induced transparency, fano resonances, and negative index of refraction. Such superstructures offer great potential in nanoscopic light shaping, optical signal processing, optical manipulation, holography, and transduction. Together with the works on applications of complex shaped metal NPs, there has been increasing understanding of the fundaments of the surface plasmon phenomenon including non-linear optical properties [8]. A review of the most promising applications follows.

- **Using plasmonic nanoparticles as single species.** When considering the application of metal NPs as individual entities, the first property, which comes to mind, is their extremely big absorption and scattering cross-sections. This makes them ideal candidate for biomedical labelling and imaging using reflectance confocal microscope or advantageously using dark-field scattering microscope. Beside the light-scattering capability, there are more points of interests, which make the plasmonics NPs highly desirable material for biomedical research and technologies. (i) The plasmon wavelength of plasmonics NPs can be readily tuned by shape of the particle without much changing the overall volume of the individual particle. The range of the possible frequencies ranges from visible light to near infrared. The NIR region is especially important for biomedicine applications [2]. (ii) The plasmon effect is highly resistant to photo-bleaching – an effect commonly battled with in biomedical imaging when using fluorescent dyes. (iii) The metal NP surface could be functionalized with surface chemistry to be specifically targeted to various proteins/objects in biological systems [9]. A brief list of the most common application fields for the single metal NPs follows:
    - Shape dependent markers for electron microscopy
    - Labels for diagnostics and therapy in biotechnology
    - Plasmonic photothermal conversion (theranostics)
    - Laser welding
    - Plasmonic sensing

    - Plasmonic nanoantennas
- **Plasmonic nanoparticle assemblies:** The overall action of a NP ensemble, the arrangement of plasmonic NPs into oligomers large scale ordered two-dimensional or three-dimensional superstructures, can exhibit potentially various attractive properties arising from simultaneous contribution from the individual NPs and the collective inter-particle LSPR modes. When metal NPs are placed adjacent to one another, their localised plasmon resonances are coupled through electrostatic interaction. This plasmon coupling can be viewed as an analogy to hybridization of molecular energy states and can span from simple dimers to plasmon modes encompassing whole arrays of NPs and propagating surface plasmon resonance. These collective modes brings many interesting collective plasmon responses, such as extreme electric field inside the particle gaps, distinct collective modes, and exotic fano resonances [10]. For NP of complex geometries (thus reduced axes of symmetries) like AuNR, the collective plasmon responses from their assemblies are further enriched due to the anisotropic optical response of the individual particles [1, 7]. These novel properties are favourable and are key to many outstanding optoelectronic and biomedical applications. Such structures often fall within the meta-material classification [11].
- **Cross-over applications:** Not all utilisation of noble metal NPs can be categorised as single-particle or interacting particle assembly. There are of course applications utilising the optical properties of metal NPs in large ensembles, where the multiplicity of NPs only adds to an overall single-particle effect. Such applications span from filters, to novel liquid crystals [12]. A brief list of the most common application fields for the single metal NPs follows:
    - Induced reversible plasmonic particle assembly in solution [13]
    - SERS markers and substrates [1]

2 AIM OF THE DOCTORAL THESIS

The thesis is a continuation of my Master's project, which dealt with metal particle nanostructures. One of the reasons why I have chosen this topic (i.e. the material- chemical point of view) is an effort to explore a material approach which involves physical engineering with the utilisation of colloidal chemistry for the preparation of anisometric plasmonic noble metal nanoparticles (NPs) with narrow size distribution. The model example of such structures is the famous gold nanorod (AuNR), a golden NP in the approximate shape of sphere-capped cylinder. Such shape has been foretold to have anisotropic optical properties early in the 19th century by Gans. However, it took almost a century to realise the golden shape experimentally in the nanoscale. At the beginning of the new millennium, three separate research groups in the world reinvented a specific synthesis for the preparation of AuNRs. The method known as seeded growth and golden nanorods as its products and applications are the focus of the thesis.

The aim of the thesis was the shape-controlled synthesis of plasmonic nanoparticles and their prospective applications. As a prototype for the entire field, gold nanorods were chosen, for their anisotropic optical properties, and great tunability in the visible and near-infrared region of the electromagnetic spectrum. As a synthesis method, seeded growth method in the presence of silver nitrate was chosen. The method gives unsurpassed yield of the rods and is a gate to many modification of synthesis for other anisometric shapes.

3 METHODS

In the course of the thesis, colloidal solutions of gold NPs (dominantly AuNRs) were characterised by UV-VIS-NIR absorption spectroscopy and electron microscopy. Both are standardized and well accepted characterization methods in colloidal noble metal NP community [1, 14]. Figure 3.1 depicts the information about the colloidal solution of AuNRs, which can be obtained using those two methods. Single AuNR exhibit two LSPR modes, which are perpendicular in polarization, as depicted in Figure 3.1-a, b. However, this anisotropic optical property is blurred in the colloidal solution where all particles constantly undergo translational and rotational movement due to the thermal motion of the solvent molecules. As a result, the absorption of the AuNR colloidal solution is spatially isotropic and exhibits both LSPR modes simultaneously. Those modes, depicted in Figure 3.1-c are called the transversal LSPR mode ($\mathrm{LSPR_T}$) and longitudinal LSPR mode ($\mathrm{LSPR_L}$), and correspond to the transversal, respectively longitudinal oscillations of the electron gas on the nanorod (Figure 3.1-a and Figure 3.1-b, respectively). The topological information on the mean shape, yield, and size distribution of the NP ensemble is acquired using the electron microscopy (EM) imaging, and the analysis of sufficient amount of particles in the EM micrographs (Figure 3.1-d). This analysis yields the mean particle sizes with the spread represented by standard deviation, which can be used to estimate the solution optical properties via numerical simulation (Figure 3.1-c).

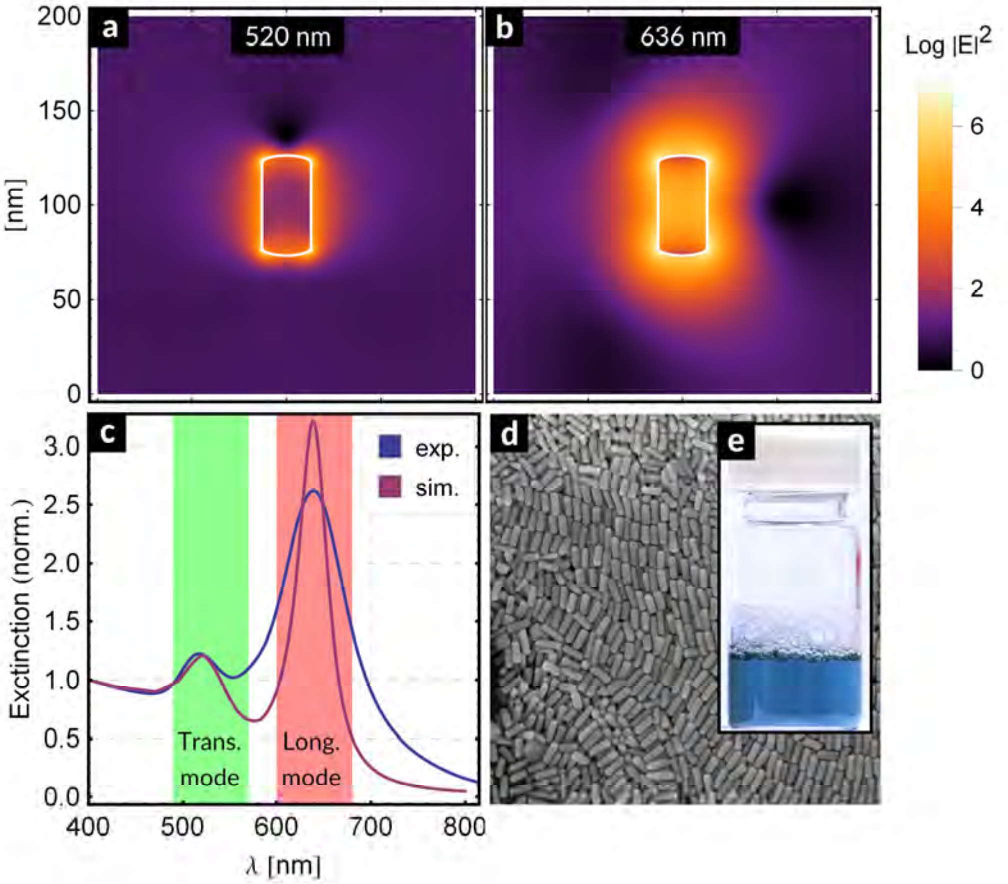

Figure 3.1: Overall picture of the optical properties of AuNR colloid. (a) BEMAX simulation of the transversal LSPR mode of AuNR. (b) BEMAX simulation of the longitudinal AuNR mode. (c) Comparison plot of the experimentally measured extinction spectra of AuNR solution and BEMAX simulation of extinction of single AuNR whose dimensions match the mean dimensions of the AuNR ensemble in the measured solution. (d) SEM micrograph of the analysed AuNR sample with the photography of the AuNR colloid in inset (e).

4 RESULTS

4.1 Electron microscopy holder for the preparation of colloidal samples

The main instrument for the characterisation of the colloidal samples was the JEOL JSM-7500F field emission scanning electron microscope (FE-SEM). The optimal conditions found for this specific instrument and specimen are imaging at accelerating voltage of 7 kV, 8 mm of working distance with the in-chamber back-scattered electron detector. For the particle size distribution analysis, the sample was prepared on a TEM grid and attached to the custom-made TEM grid sample holder (Figure 4.1), which lowers the BSE background by providing free space for the electron beam passing through the thin sample. The grid was designed and produced in collaboration with assistant Professor Jan Hošek, Faculty of Mechanical Engineering, CTU in Prague.

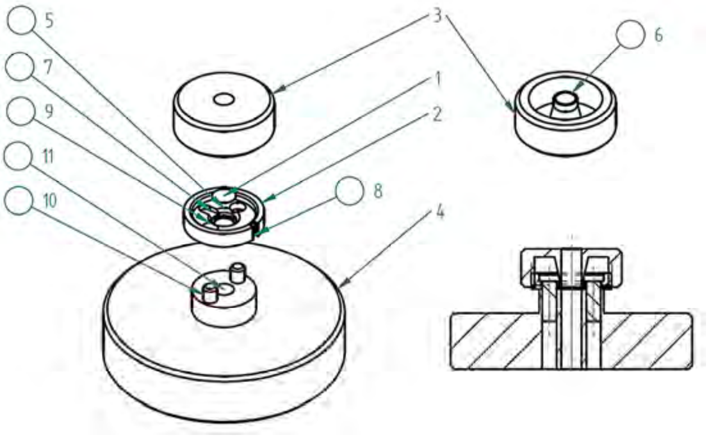

Figure 4.1: Custom made TEM grid sample holder for the observation of colloidal particles in FE-SEM JEOL-7500f. (1) TEM grid, (2) inner segment of the holder, (3) press-on outer segment of the holder, (4) assembly help adapter, (5) recess for the grid with leading countersink, (6) contact front face of the outer part of the holder, (7) path for tweezers, (8) opening for the passing of gas during evacuation, (9) openings for the pins, (10) pins on the assembly used for screwing the two parts together, (11) opening for the passing electron beam.

4.2 Software tools for microscopic image analysis and segmentation

The particle shapes and sizes are acquired from EM images taken by FE-SEM or TEM. The images are either hand-analysed or a custom developed software package is used for automatic particle measurement. Most of the colloidal samples discussed in the thesis are seeded grown AuNRs, which contain mostly rods, and in small fraction spheres and other shapes. Therefore, the image analysis divides the particles into two groups, rods and spheres, where spheres account for all the unwanted shapes.

The developed *Mathematica*™ tools consists of two parts. First, the application called ImageExplorer is depicted in Figure 4.2. To the end-user, the application looks similarly as the common applications with all the controls located at the top ribbon in the forms of icons. The application is in fact a custom styled *Mathematica*™ notebook, which contains all the needed custom functions and procedures together with the user interface code. Thus, a very handy feature emerges: the ability to save the notebook with all the variables localised and stored within. The user can start to work on an image and save it in the middle of the work, to return to it later, or to save the measurements for future reference. In its present version, the ImageExplorer app automatically imports the scales for JEOL SEM images and TEM images acquired from GATAN camera.

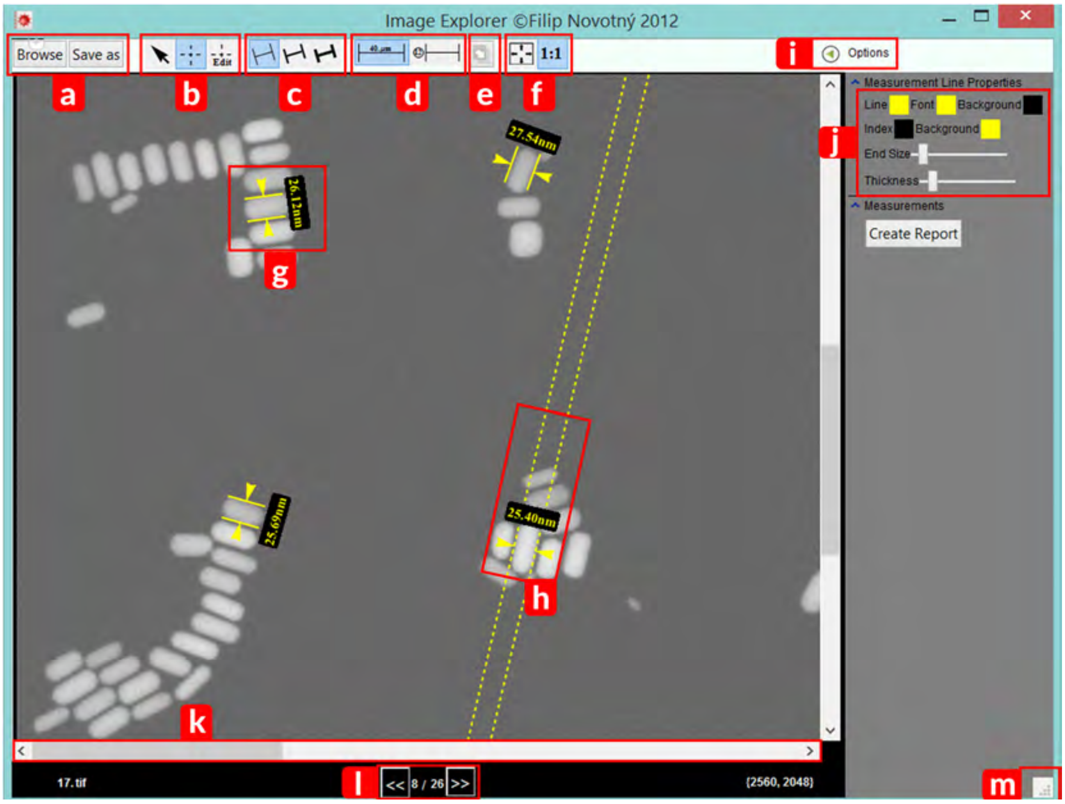

Figure 4.2: An overview of the ImageExplorer application GUI. The application focus on streamlining common tasks needed for micrograph analysis: (a) browsing for image file through system dialog & saving the image with annotations, (b) three working modes including general selection mode with access to *Mathematica*™ draw pallet; measuring mode with ability to take multiple scaled line measurements; measurement edit mode allowing for deleting or modification of already displayed measurements; (c) measurement line quick styling buttons, (d) switch to display measured lengths and measurement index for each measurement, (e) button for copying the actual values of measurement into systems clipboard, (f) image resize actions allowing for 1:1 or fit screen options, (g) measurement line adding by simple mouse click-drag-release action, (h) guiding parallel lines while entering new measurement, (i) button for hiding/unhiding the options pallet (default is to hide the pallet), (j) options for detailed styling of the measurement line a annotations, (k) scrollbars for navigating the image if 1:1 options is selected and the image is larger than the application area, (l) browse through directory capability allowing for going through all the images in the active image directory, (m) the ability to resize application window as needed – the app default starts in full screen.

Commonly, colloidal NP ensembles are characterised using TEM imaging, a method, which gives resolution surpassing the needs of the sole characterisation and supreme signal-to-noise ratio. This produces sharp smooth micrograph of NPs viable for immediate processing by computer vision. As the NP technologies evolve, there is however the need for the ability to characterise particle size distribution on arbitrary substrates such as glass of quartz – which make the utilization of TEM impossible. Modern field emission scanning electron microscope made a big leap in their abilities regarding the resolution at low- or non-conductive samples, which is also the case of NP deposited on glass or quartz. However, the image quality is far from the TEM camera, thus, additional image filtering is needed.

The custom ParticleRecognition app is designed around a practical workflow segmentation of the process of resolving a counting the particles and their dimensions in a microscopic image. The workflow is divided into five steps and is depicted in Figure 4.3.

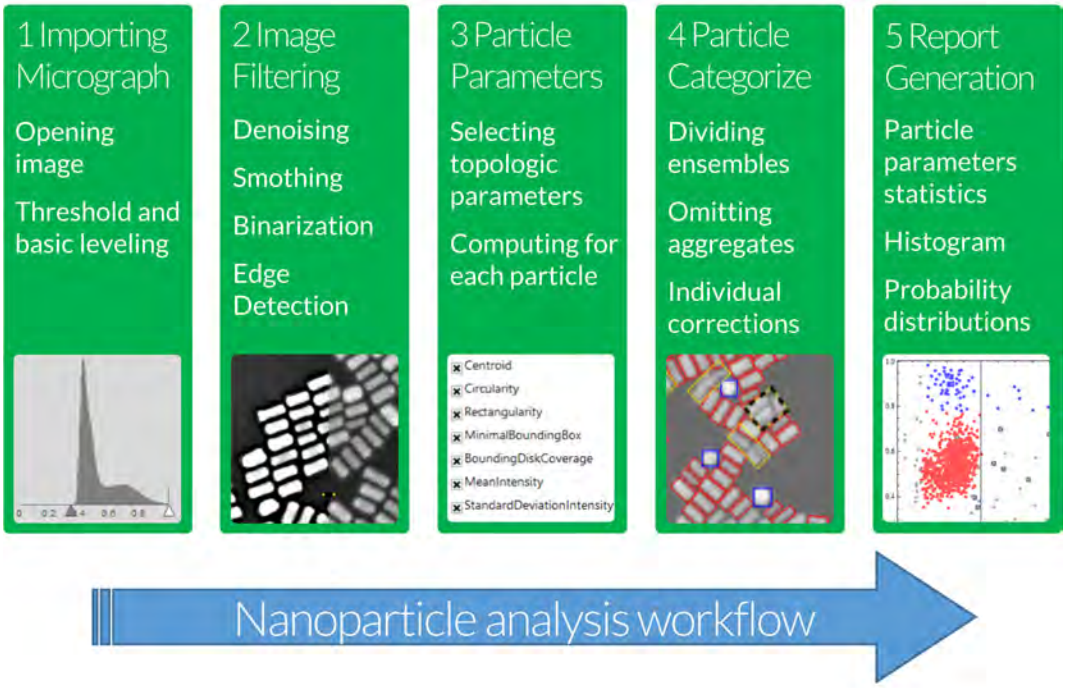

Figure 4.3: An overview of NP analysis workflow, which is the fundament under the design of ParticleRecognition app. The process of resolving particle in electron microscope image and categorising them in regards to their topological parameters is divided into five steps: (1) importing the desired micrograph and its basic setting of image levels, contrast, etc. (2) Image filtering to denoise and smooth the image while retaining the particle features. Binarization be tresholding or edge detection. (3) Determining which of the topological parameters to resolved segments of the image. (4) Categorization of disjunctive particle ensembles by selecting intervals of topological parameters in which the particle belongs. Omitting of aggregates or badly resolved images using either parameter interval or handpicking. (5) Report generation of particle distribution, mean, and standard deviations for desired particle parameters.

The above-described workflow for NP analysis is optimal for finding the right parameters for concrete micrographs taken under specific conditions. The whole idea of the ParticleRecognition app is to give a comprehensive interface to quickly process new samples. As soon as the optimal parameters for the analysis are found (the settings of image filtering methods, the selection of the topological parameters to compute, and the settings of the intervals in the parameter space, which can resolve different types of particles), the whole process can be easily simplified and automatized. This is done by exporting the found parameters into one overall *Mathematica*™ command, which is applied to a batch of images, The results are then reviewed in similar fashion to the fourth ParticleRecognition

App (Figure 4.4). There the correctness of the analysis can be checked and if necessary, the corrections can be made quickly by hand selecting the errors.

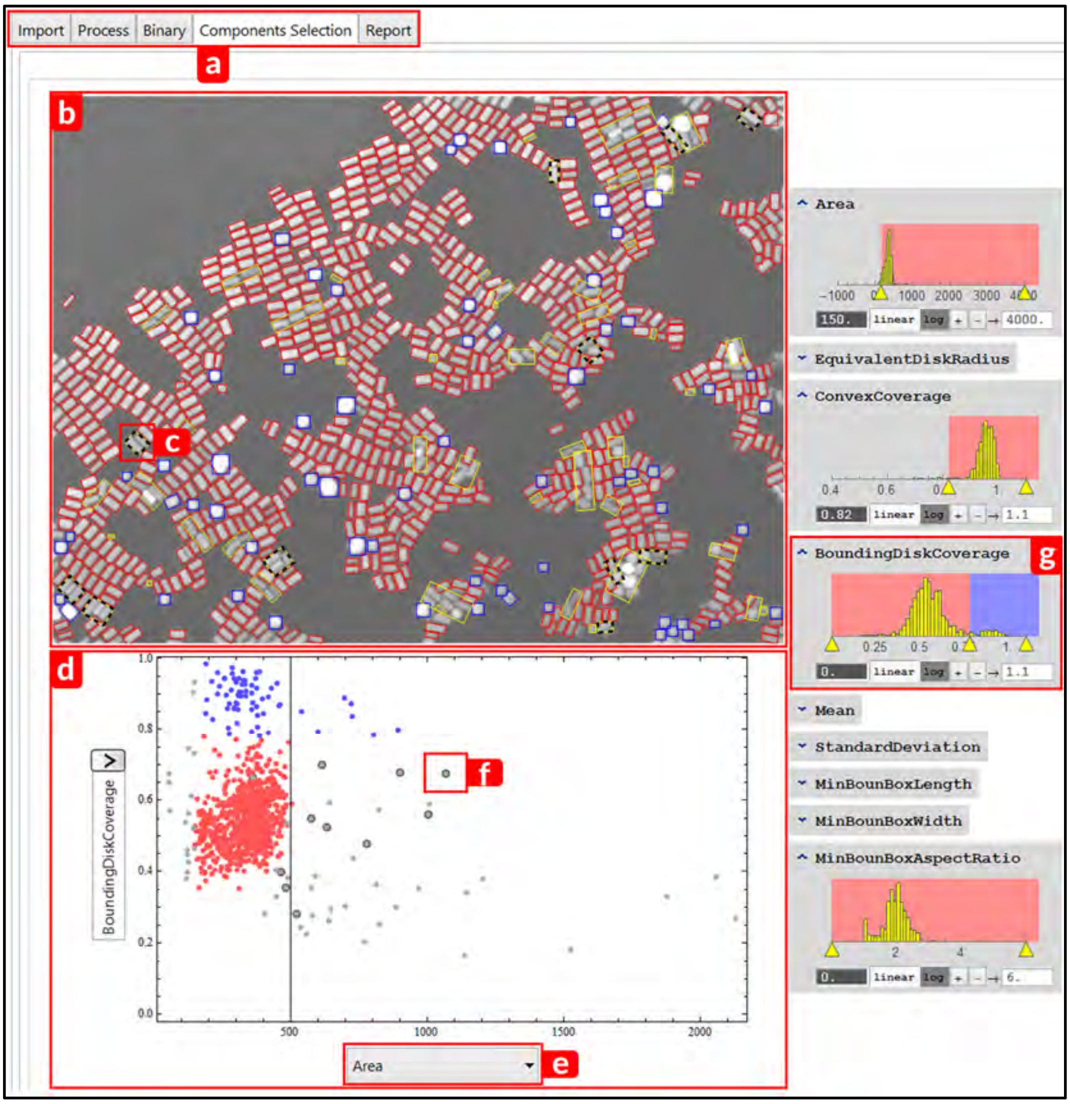

Figure 4.4: Fourth panel of the multipanelled GUI called "Components Selection". Here the user has the power to select multiple particle ensembles based on their respective parameters and handpick some particle to omit them from the measurement completely. The controls consist of: (a) the panel switcher, (b) the main interactive area consisting of the original image with overlaid boxes of detected particles. The boxes are coloured depending on which interval of values the particle fits. The red ones belongs to first set of parameter intervals, the blue belongs to second set of parameter intervals, and the yellow one are particles omitted from measurement. (c) The image area can be directly interacted with by clicking on any of the particle, to omit it manually from the measurement. (d) Second interactive area consisting of point plot of selected parameters of the particles. Here user can review the distribution of each particle type in the parameters space and hand-select particle to omit by directly clicking on each some of the points (f). (e) The parameters can by changed in real-time. (g) Main control area providing an interactive control over any selected particle parameter in for of vertical sliders with histogram chart depicting distribution of the respective particle parameter over the whole interval. User can move the slider to desired values while observing the change in the distributions of the different particle ensembles in interactive areas (b) and (d). User can also use the control (g) to split the main selection interval in more subintervals allowing for creating multiple ensembles of particles.

4.3 Calibration of [Au]/[AA] ratio

The ability to determine the amount of the ascorbic acid in excess to the amount needed for the Au^{+3} to Au^{+1} reduction is crucial for good control over the particle parameters. It has been shown convincingly that the particle shape and shape purity is strongly influenced by the reduction dynamics of the Au^{+1} species to the growing gold seeds. The precise control over the amount of AA needed to reduce Au^{+3} to Au^{+1} is challenging as some of the reactants adsorbs on the sides of the reaction vial. Therefore, to determine the reduction of gold and the excess of ascorbic acid present in the growth solution I developed protocol based on UV-VIS absorption spectra measurement.

Figure 4.5 depicts a practical example of the method to calibrate the real amount of AA to reduce the Au^{+3} in CTAB water solution to Au^{+1}. The basic idea is measure the absorbance of the growth solution without any AA added and then stepwise add small amount of AA to the solution while measuring the absorption spectra after each addition and controlled homogenization of the solution. Then extracting the absorption values of the Au^{3+} peak and extrapolate their succession by fitting by linear function to find the amount of AA needed to get the absorption to zero. I determined that the differences of the amounts of AA needed to the transformation of Au^{+3} to Au^{+1} is usually in the interval of 1% to 10% of the excess AA needed, depending on the type and size of the container.

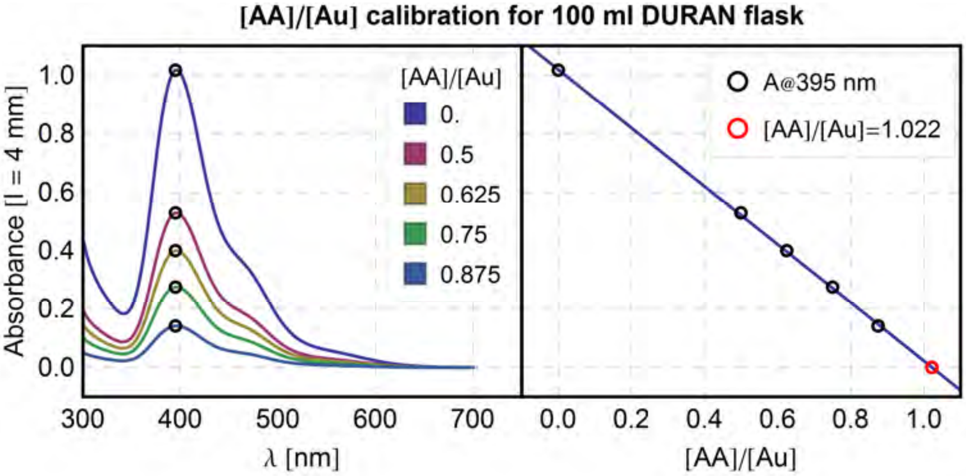

Figure 4.5: Example of the [AA]/[Au] calibration procedure for a 100 ml DURAN flask. (left) Absorption spectra taken at different fractions of AA added into Au/CTAB/water solution. The real amounts equals to 0 µl, 200 µl, 250 µl, 300 µl, 350 µl respectively of 0.1 M AA added to ~80 ml of ~0.5 mM Au solution. (right) Fitted spectra peaks (taken at λ = 395 nm) with line fit and extrapolated crossing of the fitted function with Absorbance = 0. The extrapolated zero crossing equals 1,022 which is transformed into 408,8 µl of 0,1 M AA to fully reduce the Au^{+3} to Au^{+1} (8,8 µl excess of what was expected).

4.4 Formulation and utilization of a growth initiation step

The absorption kinetic experiments showed that splitting the full amount of AA added into the growth solution into smaller amounts have the effect of improving the AuNR solution quality and aspect ratio of the rods. However, still the stepwise additions caused changes in the growth model indicated by the "bumps" in the kinetics data. In the sense of the formulated additional step of initiation, this kinetics experiment can be directly rephrased into its context – the initial excess of the AA present at the beginning of the synthesis induced the growth initiation and the stepwise adding of AA formed the third growth stage.

A demonstration of the utilisation of the results from absorption kinetics follows. The experiment consists in exploring the growth of the rods in the presence of CTAB in concentration one order of magnitude lower than in original protocol (10 mM instead of 100 mM). Although it may appear that the colloidal solution of AuNRs seems to acquire its production costs mainly from the amount of gold, it is CTAB, which presents the main costs in the synthesis process. Its high concentration (0.1 M) surpasses the concentration of gold salt used (0.5) by three orders of magnitude.

Since the beginning of the studies of the initial seeded growth protocol with the CTAB as the surfactant, there were studies to explore the effects and propose way how to lower its enormous amount needed for the high yield synthesis. Diluting the CTAB concentration fifty times to 0.02 M produces polydisperse, mainly spherical, particles with large number of prolonged particles possibly created by sintering of the spherical ones.

The behaviour of the seeded growth synthesis at very low CTAB concentrations (10 mM) while utilizing the knowledge from the absorption kinetics experiments can be explored further – initiation at low amount of excess AA and then controlled gradual addition of AA by syringe pump to govern the growth kinetics of particles in the solution. Figure 4.6 contains result of such synthesis, the characterisation of AuNRs produced at 10 mM CTAB concentration. The above-described experiment produced by all standards reasonable quality rods with following parameters: The mean dimensions of the rods are (42.0 ± 4.9) nm of length and (20.8 ± 2.9) nm of width. The mean aspect ratio is (2.04 ± 0.27). The respective percentages spreads of the parameters are 11.75%, 13.98%, and 13.17%. The yield of the rods is 91.58% of all particles counted.

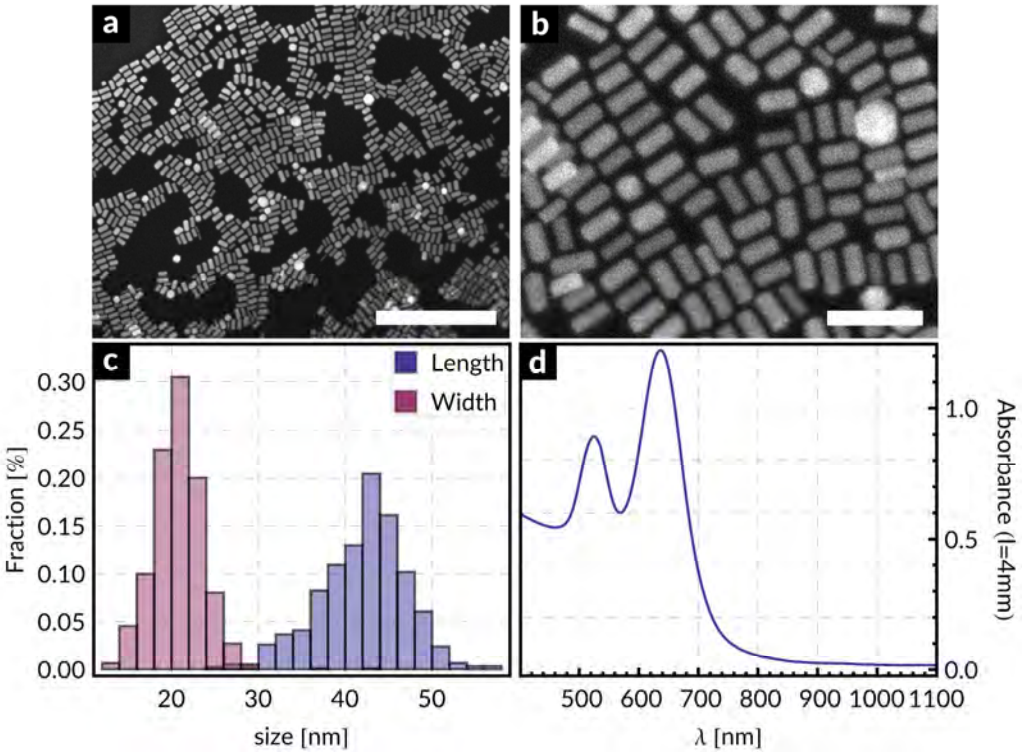

Figure 4.6: Characterisation of AuNRs sample produced in low CTAB concentration (10 mM). (A-B) SEM image of the prepared rods. (C) Histogram chart of the distribution of lengths and widths of the rods in the analysed sample. (D) Absorption spectrum of the analysed sample.

This is an excellent result when compared to the quality of the rods produced by standard seeded growth approach under the condition of low CTAB concentrations. In addition, it was achieved with 10 mM CTAB concentration, which is ten times lower than usual. The only parameter, which is worse than what would be in standard, seeded growth protocol with 0.1 M CTAB is the yield of the rods, which in the standard protocol tends to be around 96+ %.

4.5 Gold nanorod arrays study and visualization

The pioneering works on AuNR self-assembly observed that on of the main factors governing the AuNR@CTAB self-assembly is the [Au]/[CTAB] ratio during the supracrystal formation [15, 16]. The formulation of such parameter is tricky as the concentration of both species changes during the evaporation of colloidal drop and in addition, the distribution both the AuNRs and CTAB is not homogeneous during the drying process. However, it was showed that at certain [Au^0]/[CTAB] ratio, the self-assembly process results in bigger, more ordered domains.

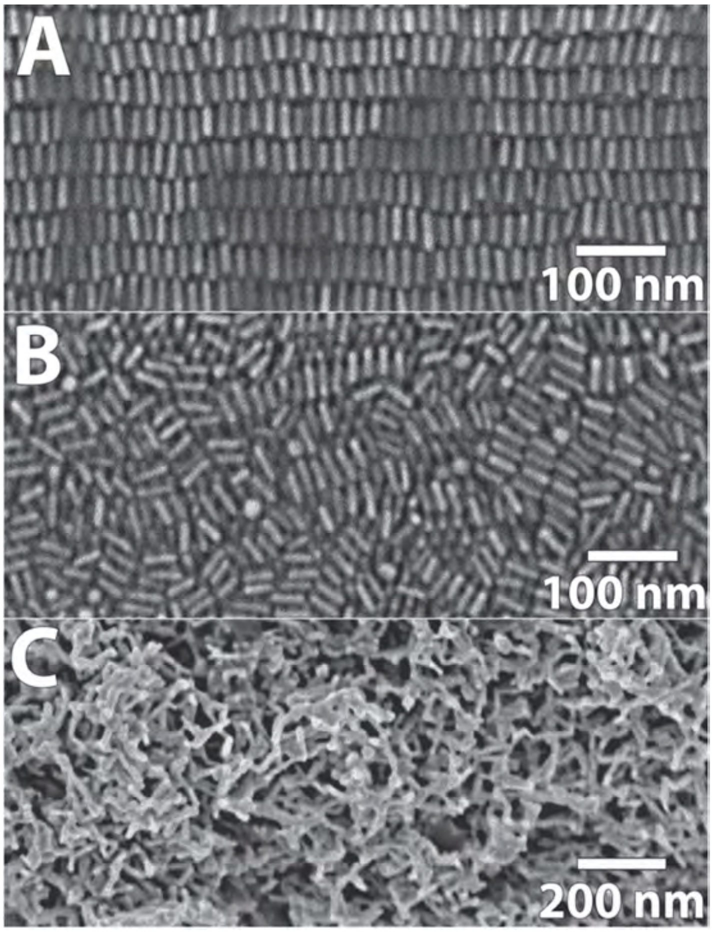

Figure 4.7: Demonstration of the various self-assembly levels attainable by changing the [Au^0]/CTAB ratio. The parameter goes from 8 to 13, and to 80 in the A,B,C sub-images respectively. Reprinted from [17].

We exploited that approach and analysed the process of AuNR self-assembly by colloidal droplet evaporation in similar fashion including temperature and the addition of non-polar solvents. The results were assembled depending on the quality of the ordered AuNR regions in terms of area of the self-assembled rods and the size of individual crystal domains. We found the optimal condition for the AuNR@CTAB self-assembly to be 40°C and the [Au^0]/[CTAB] ratio to equal 8. In the following experiment demonstration, these would be the base parameters where to start. Figure 4.7 shows the effect of the [Au^0]/[CTAB] parameter on the ordering of AuNR in the deposited colloidal material.

The FEI&CSMS stipend for young researchers using electron microscopes provide me with the opportunity to collaborate with the electron microscopy experts at FEI. We utilised an advanced technique environmental scanning electron microscope in scanning transmission electron microscope (ESEM-in-STEM). Together with the microscope operator Petr Wandrol we utilised the setup for in-situ study of the events taking place in the drying colloidal droplet of AuNR/CTAB/water solution. The experimental approach is schematically depicted in Figure 4.8, and consists of equilibrating a droplet of AuNR colloidal solution on the WetSTEM holder assembly and the introducing it into the ESEM chamber. There, suitable conditions of formation and visualization of thin viscous film of AuNR/CTAB/water on the holey carbon TEM grid are set, and the STEM technique allows visualizing the system in the wetted state.

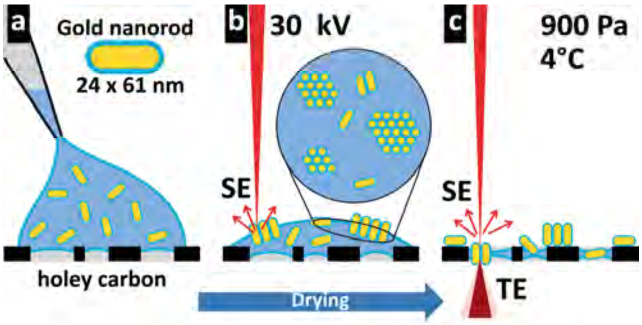

Figure 4.8: Scheme of in-situ observation of self-assembly of colloidal AuNRs. (a) Nanorod solution is deposited on top of a holey carbon TEM grid situated in the WetSTEM block. (b) Droplet undergoes rapid evaporation under the controlled conditions inside ESEM chamber. The droplet collapse is monitored by secondary electron (SE) detector at low magnification. (c) Collapsed drop concentrates the AuNR/CTAB volume to form a hydrated viscous CTAB/water membrane transparent for transmitted electron (TE) signal at high magnification. Single-particle resolution is achieved. Reprinted from [18].

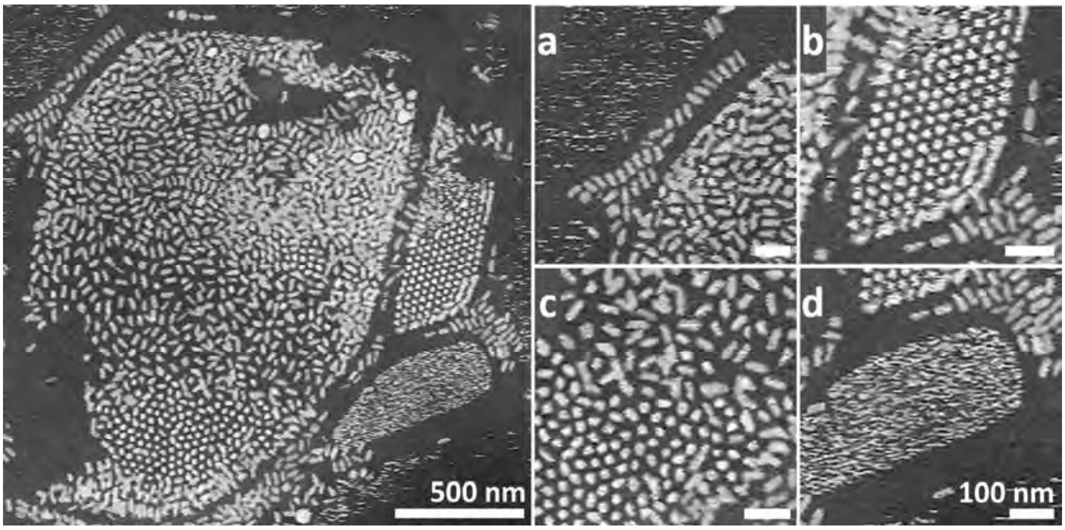

Figure 4.9: Overall picture of the self-assembly in action (left, bar = 500 nm). (a) A twisted chain of AuNRs formed by action of merging their CTAB solvating double-layers into a twisted worm-like micelle (Scale bar = 100 nm). (b) Free-standing AuNR arrays can be clearly seen (Scale bar = 100 nm). (c) Also, metastable situation of forming array with loose packed rods (Scale bar = 100 nm). (d) Noisy areas correspond to thermal motion of the rods being too quick in the terms of scan rate (Scale bar = 100 nm). Reprinted from [18].

By such approach, we were able to study the system used by the pioneer work in AuNR self-assembly in-situ. The main result of our observation using WetSTEM technique can be refined into a single image depicted in Figure 4.9.

4.6 Ordered gold nanorod monolayers and their optical properties

Our AuNR deposition setup consists of continuously pumped desiccator vessel filled with redistilled water and equilibrated at 30 °C. The continuous evacuation creates high-humidity environment close to the point of saturated vapours and low pressure approximately 4000 Pa. The setup overview is depicted in Figure 4.10. The desiccator was used as a vessel for creating more controlled environment than closed petri dish. Although crude, the setup allows for non-trivial thermodynamic condition of high humidity environment in low pressure. If the conditions are stable, the particles self-assembly into ordered arrays via the steric interactions and the minimization of the surface area. In the case of rods, the most efficient configuration is the self-standing array of vertically packed rods perpendicular to the gas/liquid boundary.

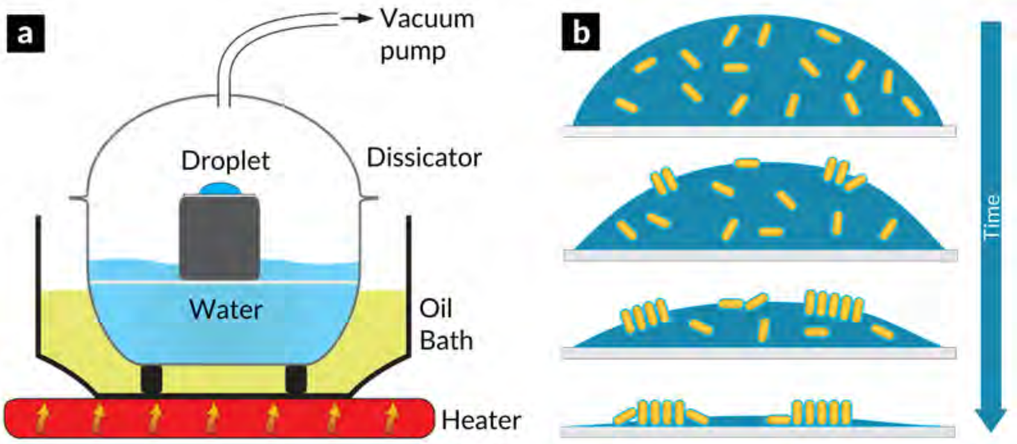

Figure 4.10: A schematic overview of setup for 2D AuNR arrays preparation. (a) The laboratory setup consists of desiccator vessel with the sample located inside at heightened place. The vessel is filled with water to provide saturated water vapour environment. The desiccator vessel is connected to vacuum pump for limited control of the inner atmospheric conditions. Whole sample assembly is in oil bath for the control of temperature. (b) A schematic illustration of the AuNR self-assembly process from by rapid evaporation of a colloidal droplet. The flow created by water evaporating from the droplet surface concentrate particles at the water/air boundary. At certain conditions, nucleation of vertical standing AuNR arrays takes place. Such structures are then deposited on substrate upon complete evaporation of the sample.

The vertically stacked 2D AuNR arrays are sufficiently thin to explore their properties in transmission optical microscope. When observing the self-assembled sample from section under the transmission optical microscope, immediately colourful areas can be seen. By correlating the two images it can be derived that the black absorbing areas of the optical image corresponds with the small voluminous stacks and the blue-red areas corresponds to the AuNR monolayer consisting of the vertical 2D AuNR arrays and loosely lying rods.

Figure 4.11 shows a correlated optical microscope / SEM analysis of an area of the self-assembled AuNR domains. The sub images Figure 4.11a-d and Figure 4.11e-f forms two close-up imaging of the selected AuNR islands, whose differ in the relative colour in the transmission optical microscope. From SEM the detailed SEM images are immediately apparent the main difference between the two islands is the orientation of the rods inside the crystal.

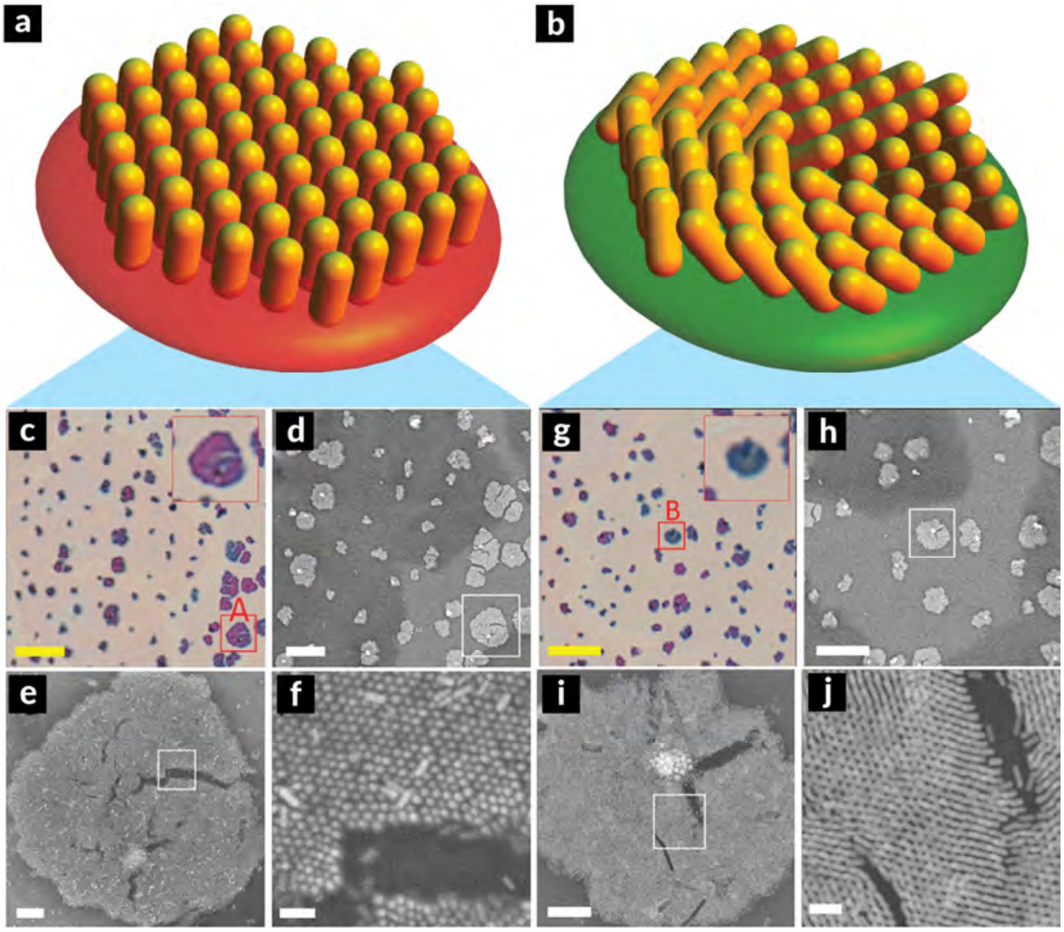

Figure 4.11: Correlated optical microscope/scanning electron microscope study of the self-assembled vertically stacked AuNRs: (top-left) The apparent violet colour of the AuNR assembly and (a - d) its SEM micrograph showing the rods are mainly in upright position. (top-right) Similar imaging on other AuNR domains, which exhibits greenish appearance under optical microscope. (e - h) The rods conformation in this case is changed significantly, as the rods are angling from the vertical axis with different directions. Interesting circular patterns can by identified in the collective AuNR orientation. The optical change is not trivial to discuss as it was shown the LSPR of individual AuNRs form collective resonant fields at such close spacing [5]. The apparent colour of the individual AuNR islands is dependent on the rod orientation, number of stacked layers and on interparticle distances. Scale bars: (a,e) 10 mm, (b,f) 5 mm, (c)2 mm, (g) = 1 mm, (d,h) 100 nm.

The rods in the 2D island whose colour appear to be violet (Figure 4.11a) are nearly straight up standing, whereas the rods in the island which appear green (Figure 4.11b) are leaning of the vertical axis as depicted on the visualizations in Figure 4.11top-left and Figure 4.11 top-right. This is a demonstration of the sensitivity of the optical properties of ordered arrays of anisometric plasmonic NPs. For exact analysis, a spectroscopic measurement is needed together with simulation of the presumed structure by any of the possible methods for computing the optical properties of metal nano-arrays. Such endeavour is of out of the scope of the thesis. This simple demonstration is mainly meant to show the possibility to assess the quality of the AuNR self-assembly by optical microscopy.

4.7 Voluminous gold nanorod supracrystals and their optical properties

The preparation of voluminous AuNR supracrystals was achieved by controlled drying of small amount of AuNRs concentrate on glass substrate, where drying near the liquid was kept stable by forming space volume between the substrate, and microtome knife, within which the AuNRs concentrate, was held. This was done by forming planar capillary between glass substrate and microtome glass knife, as depicted in Figure 4.12. The knife can be moved in XYZ direction by micrometre screws, to obtain ideal shape of the meniscus. This setup allowed holding the meniscus line stable as long as possible as the volume of AuNRs concentrate was going smaller. The ability to control the thickness of the formed planar capillary (the height of the knife-edge above the substrate) proved to be critical. Therefore, a camera with macro lenses was added to calibrate the actual capillary width.

Scheme at Figure 4.13-a allows detailed description of the AuNR deposition process. The AuNR concentrate (~20 µl) is placed by pipette into the formed planar capillary between the microtome knife and substrate. The heater pad (~ 30°C - 40°C) stabilizes the substrate temperature. The microtome knife is dragged by linear motor to give some amount of controlling the meniscus tension. The injected AuNR concentrate concentrates further as the solvent (water) evaporates. The evaporation rate is of course dependent on the local thermodynamic parameters, the knife effectively limit the surface from which the evaporation takes place.

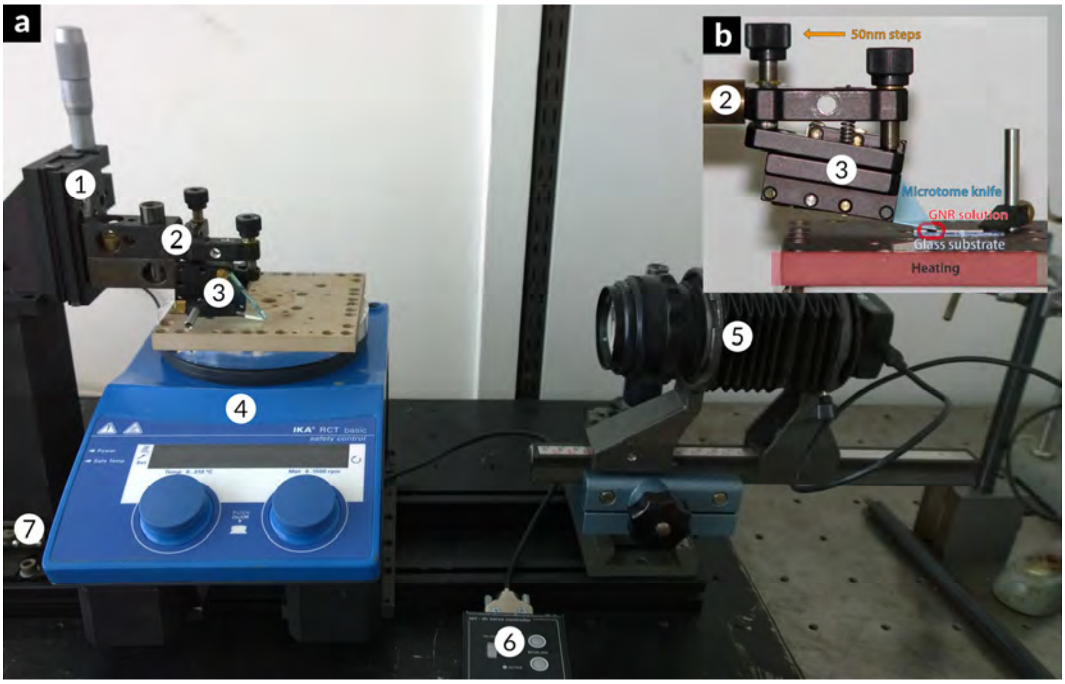

Figure 4.12: Photograph of the deposition setup with highlighted parts. (1) XYZ micrometric screws for precise positioning of the microtome knife above the substrate. (2) the microtome knife assembly attached to the assembly connected to linear motor. (3) Attachment of the microtome knife allows for setting angle along the longer and short side of the knife for levelling above the substrate. (4) heating pad with feedback loop for temperature stabilization. (5) Camera with macro lenses assembly for calibration and observation of the assembly process. (6) Thorlabs linear motor driver. (7) linear motor moving the knife assembly (hidden beneath the heating pad.)

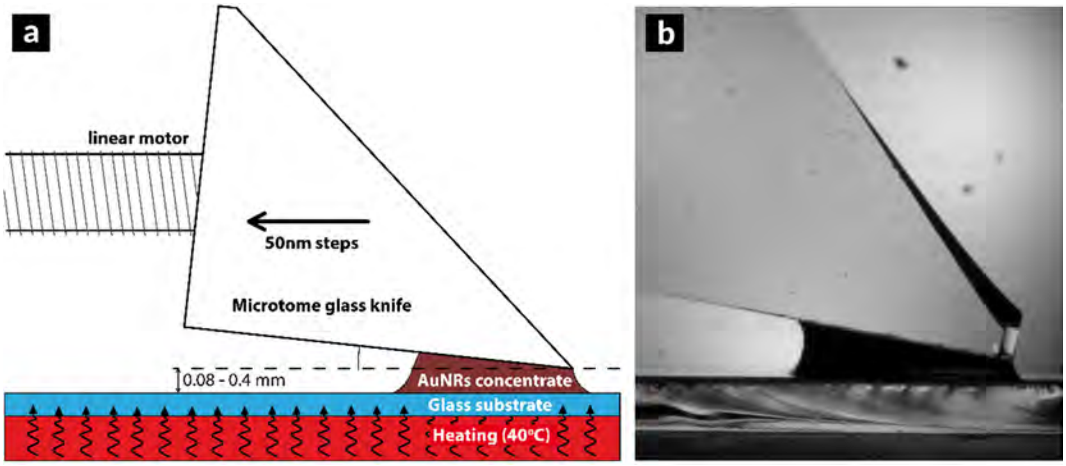

Figure 4.13: (a) An illustrated scheme of the deposition setup with (b) macrophotography of the physical device in detail.

Figure 4.14 shows colloidal crystal viewed from several distinct crystal faces together with the 3D model visualization of corresponding rod HCP-like assembly facet. The result agrees well confirming that the rods preferentially self-assemble into the HCP-like crystal.

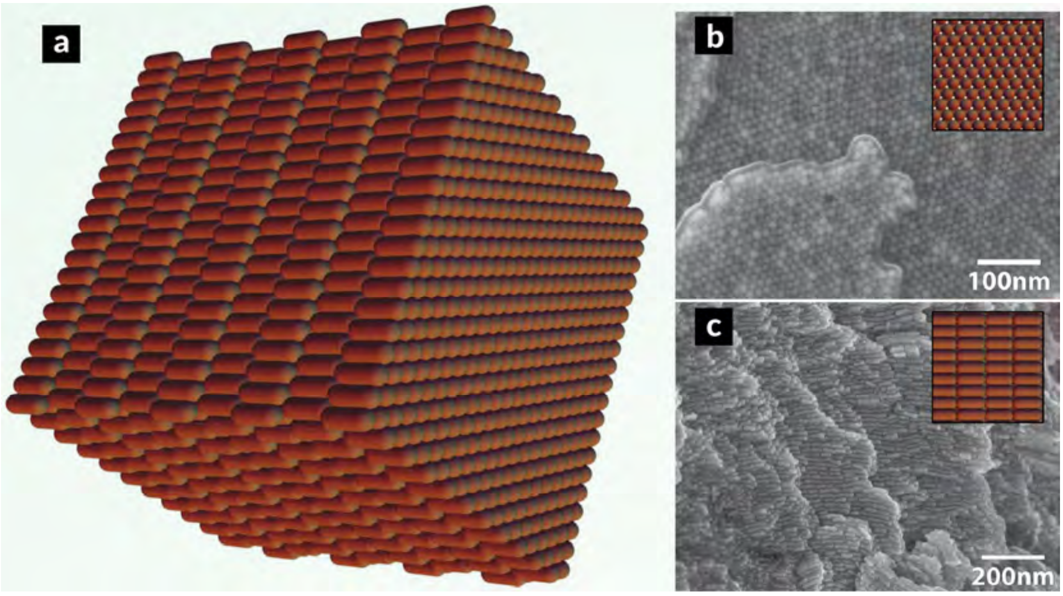

Figure 4.14: 3D model of AuNRs of aspect ratio 3.5 forming a hexagonal-closest-packing-like colloidal crystal (A) and detail SEM images of different AuNR crystal facets with corresponding projection of the 3D model.

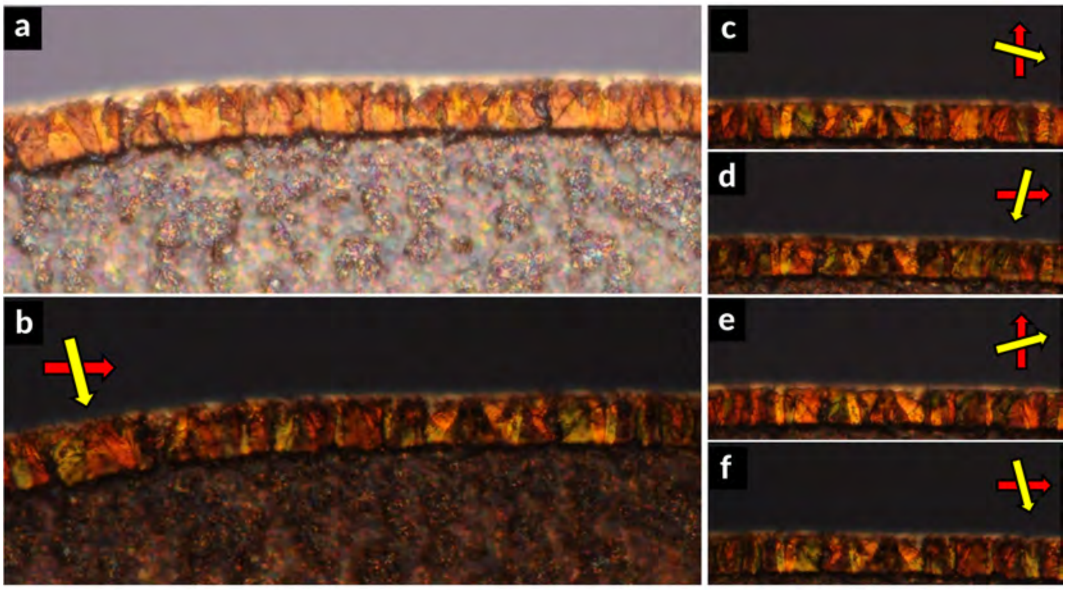

Figure 4.15: An overview of the optical behaviour of the voluminous AuNR arrays with increased interparticle spacing. (a) Wide-field reflection optical microscope image of the deposited line of voluminous AuNR supracrystals. (b) The same area visualized under the near crossed polarizer-analyser settings showing anisotropic optical properties of the distinct domains (rod) orientations present in the sample. (c - f) A selected crop of the 3D AuNR self-assembly area photographed at different polarizer-analyser settings showing the colour switching of the 3D AuNR domains. The red and yellow arrows indicates the used polariser respectively analyser setting.

Figure 4.15 shows a reflectance optical microscopy study of self-assembled voluminous AuNR domains prepared by the described protocol. The main difference to the reflectance optical microscopy image is that the imaged voluminous crystals were not let to crystallise fully to retain large interparticle distance as, an optional feature of the presented self-assembly method. The Figure 4.15-a is the microphotograph of such self-assembled domains when no polarizer setting is applied to the setup. When compared with the fully crystallised voluminous AuNR arrays, the difference in the relative colour is apparent. The golden colour turns toward brown and details in the deposited rim of supracrystals can be seen. Later in this section, it will be demonstrated that such details are in fact distinct AuNR supracrystals domains, which differs in the orientation of rods within.

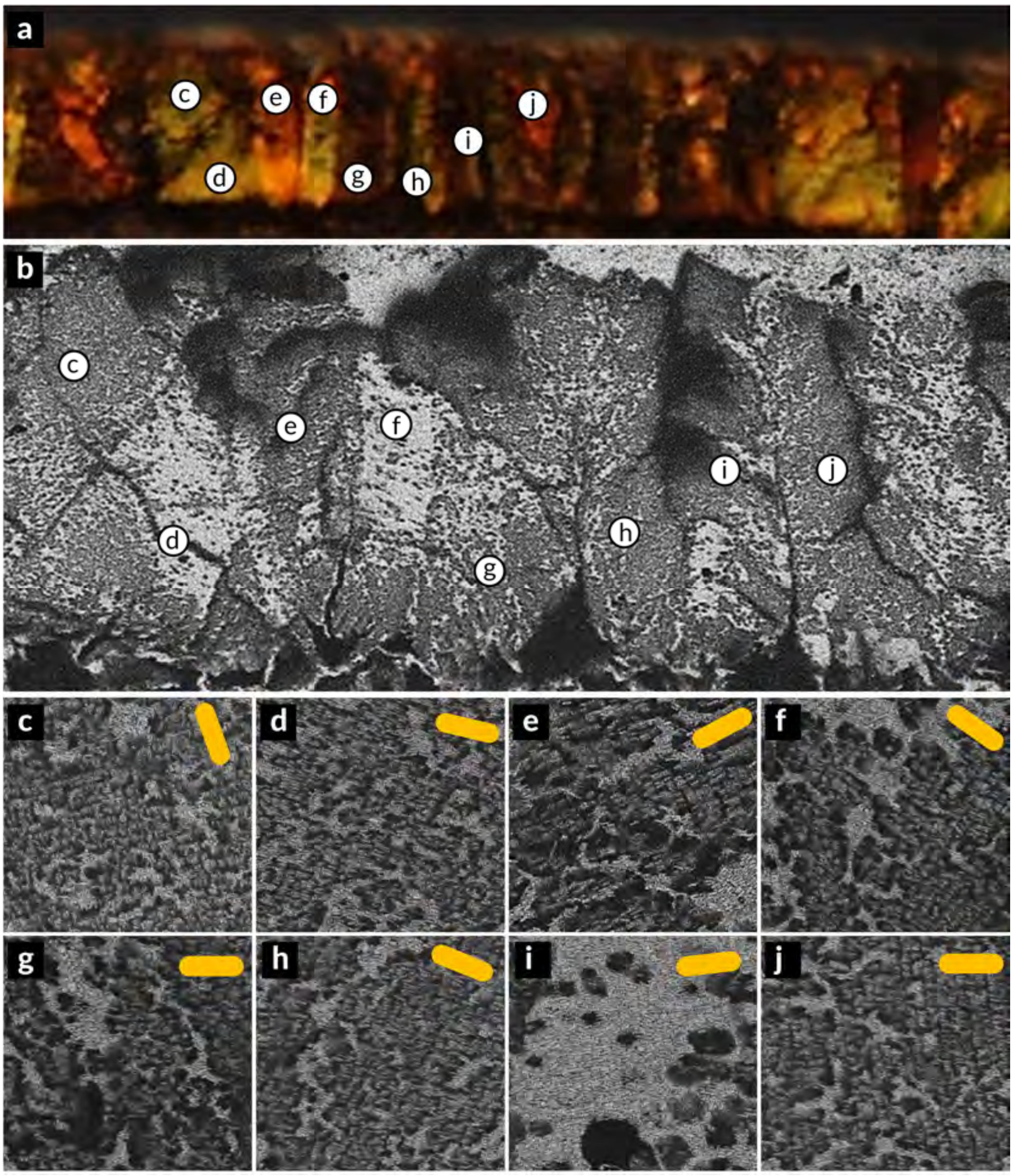

Figure 4.16: Correlated reflected light microscope / SEM analysis of the voluminous AuNR assemblies. (a) Reflection optical image of the analysed area with depicted distinct domains c-j. (b) FE-SEM image of the analysed area. The optical and FE-SEM image can be connected by the topographical features. The letters c-j indicate the identical domains on both the optical and FE-SEM image. (c-j) details of the selected voluminous AuNR domains where the overall orientation of the rods in the supracrystal can be resolved. The orientation is indicated by a rod sign in top-right corner of each of the detailed sub-images.

The contrast between the individual AuNR supracrystals domains is greatly enhanced when polarizer and analyser is applied to the optical path, as shown in Figure 4.15b. The contrast is biggest when one is near the crossed polariser settings; in addition, the individual domains change their relative colour upon the passing of the crossed polarisers' state. This effect is depicted in Figure 4.15c-f, where a selected area of the sample is visualised using different polariser-analyser settings. The underlying reason for this behaviour is explored in Figure 4.16 in a correlated reflection microscope / SEM study of a small area on the presented sample. The detailed SEM analysis of the supracrystals found that the difference in the relative colour of each domain is connected to the orientation of the rods within the crystal. The estimated orientation of each analysed domain is shown in Figure 4.16c-j.

4.8 Optimized protocols for gold nanorod synthesis

The result of the synthesis of colloidal metal NPs is always determined by the local laboratory conditions, including the type of the glass used as reaction vessels etc. [19]. The introduction of the calibration method for the [Au]/[AA] ratio allows for successful scaling of the synthesis; nevertheless, the exact conditions and reaction vessels are critical to reproduce the results. In the thesis, I describe developed protocols for the preparation of AuNRs targeted for biotechnological applications as follows:

- **Gram-scale gold nanorod synthesis tuned at $\mathrm{LSPR_L}$ = 633 nm.** The mean dimensions of rods are (54.0 ± 5.7) nm of length and (26.2 ± 3.6) nm of width. The mean aspect ratio is (2.08 ± 0.22). The spread of the length, width, and aspect ratio equals 10.6 %, 13.7 %, and 10.4 %, respectively.
- **Preparation of gold nanorods tuned at $\mathrm{LSPR_L}$ = 808 nm using syringe pump.** The mean dimensions of rods are (63.8 ± 8.2) nm of length and (18.8 ± 2.7) nm of width. The mean aspect ratio is (3.42 ± 0.38). The spread of the length, width, and aspect ratio equals 12.9 %, 14.5 %, and 11.2 %, respectively.
- **Preparation of large gold nanorods by tertiary overgrowth.** The mean dimensions of rods are (118.8 ± 10.6) nm of length and (66.6 ± 6.5) nm of width. The mean aspect ratio is (1.79 ± 0.18). The spread of the length, width, and aspect ratio equals 8.9 %, 9.8 %, and 10.0 %, respectively.
- **Preparation of small gold nanorods for cellular biology.** I successfully prepared small AuNRs with mean dimensions of (16.3 ± 2.9) nm x (6.2 ± 0.8) nm.

5 CONCLUSION

I have elaborated precise protocol for the preparation AuNRs, with narrow size distributions, which allows such nanomaterial to be targeted at specific applications. I build upon a known seeded growth method in the presence of silver nitrate. The method was investigated through the study of reaction kinetics. From the interpretation of the results, I defined a method for calibration of the relative [Au]/[AA] ratio, which strongly influences the growth of the particles at the beginning of the synthesis, for better control of the synthesis and for scalability of the synthesis, when changing the reaction vessels. I used the outcome of the investigations to define exact laboratory protocols for the preparation of particle types targeted at specific applications. Those protocols include: (i) small rods for cell nuclei biology; (ii) gram-scale synthesis of rods with $\mathrm{LSPR_L}$ targeted at 633 nm for use in biological microscopy setups; and (iii) synthesis of rods with $\mathrm{LSPR_L}$ targeted at 808 nm for the emerging field of theranostics. The protocols have been successfully used by collaborators and students. An example of two application: the simultaneous immunolabeling and the study of the AuNR uptake by human prostate carcinoma cells by standard biological confocal setup are presented.

I have formulated two methods for the controlled preparation of AuNR supracrystals, as a prospective approach for the technological preparation of metamaterials. I succeed in the preparation of both ordered monolayers and voluminous superstructures of AuNRs in such dimension that they can be studied using standard wide-field optical microscope. The laboratory setup needed for the methods are built at the department and free to use for researchers or students. In addition, in collaboration with experts from FEI Company, I utilized the gained knowledge to observe successfully the self-assembly of anisometric AuNRs in the drying colloidal droplet with single particles resolution. This was the first in-situ observation of this common self-assembly setup and was published in a special issue of journal of Microscopy and Microanalysis.

I developed a package for the import of proprietary spectroscopic formats into *Mathematica*™ computational software. I designed and developed applications for the analysis of microscopic images of NPs in the form of user-friendly *Mathematica*™ notebook interface. The goal was to streamline and refine the characterisation of the colloidal material, to allow a programmatic and reproducible quality control of synthesised colloids.

6 BIBLIOGRAPHY

[1] CHEN, H., L. SHAO, Q. LI and J. WANG. Gold nanorods and their plasmonic properties. *Chem Soc Rev* [online]. 2013, vol. 42, pp. 2679–724. ISSN 1460-4744 (Electronic) 0306-0012 (Linking). Retrieved from: doi:10.1039/c2cs35367a

[2] ALKILANY, Alaaldin M., Samuel E. LOHSE and Catherine J. MURPHY. The gold standard: gold nanoparticle libraries to understand the nano-bio interface. *Accounts of Chemical Research* [online]. 2013, vol. 46, no. 3, pp. 650–661. ISSN 1520-4898. Retrieved from: doi:10.1021/ar300015b

[3] LUK'YANCHUK, Boris, Nikolay I. ZHELUDEV, Stefan A. MAIER, Naomi J. HALAS, Peter NORDLANDER, Harald GIESSEN and Chong Tow CHONG. The Fano resonance in plasmonic nanostructures and metamaterials. *Nature Materials* [online]. 2010, vol. 9, no. 9, pp. 707–715 [accessed. 4. February 2014]. ISSN 1476-1122. Retrieved from: doi:10.1038/nmat2810

[4] LI, Chun. A targeted approach to cancer imaging and therapy. *Nature Materials* [online]. 2014, vol. 13, no. 2, pp. 110–115 [accessed. 8. July 2014]. ISSN 1476-1122. Retrieved from: doi:10.1038/nmat3877

[5] WANG, Y., K. C. BLACK, H. LUEHMANN, W. LI, Y. ZHANG, X. CAI, D. WAN, S. Y. LIU, M. LI, P. KIM, Z. Y. LI, L. V. WANG, Y. LIU and Y. XIA. Comparison study of gold nanohexapods, nanorods, and nanocages for photothermal cancer treatment. *ACS Nano* [online]. 2013, vol. 7, pp. 2068–77. ISSN 1936-086X (Electronic) 1936-0851 (Linking). Retrieved from: doi:10.1021/nn304332s

[6] EUSTIS, Susie and Mostafa A EL-SAYED. Why gold nanoparticles are more precious than pretty gold: noble metal surface plasmon resonance and its enhancement of the radiative and nonradiative properties of nanocrystals of different shapes. *Chemical Society Reviews*. 2006, vol. 35, pp. 209–217.

[7] LOHSE, Samuel E and Catherine J MURPHY. The Quest for Shape Control: A History of Gold Nanorod Synthesis. *Chemistry of Materials*. 2013, vol. 25, pp. 1250–1261. ISSN 0897-4756.

[8] HARTLAND, G., H. OKAMOTO, M. ORRIT and P. ZIJLSTRA. Optical studies of single metal nanoparticles. *Phys Chem Chem Phys* [online]. 2013, vol. 15, pp. 4090–2. ISSN 1463-9084 (Electronic) 1463-9076 (Linking). Retrieved from: doi:10.1039/c3cp90022c

[9] VIGDERMAN, L., P. MANNA and E. R. ZUBAREV. Quantitative replacement of cetyl trimethylammonium bromide by cationic thiol ligands on the surface of gold nanorods and their extremely large uptake by cancer cells. *Angew Chem Int Ed Engl* [online]. 2012, vol. 51, pp. 636–41. ISSN 1521-3773 (Electronic) 1433-7851 (Linking). Retrieved from: doi:10.1002/anie.201107304

[10] KELLY, K. Lance, Eduardo CORONADO, Lin Lin ZHAO and George C. SCHATZ. The Optical Properties of Metal Nanoparticles: The Influence of Size, Shape, and Dielectric Environment. *The Journal of Physical Chemistry B* [online]. 2003, vol. 107, no. 3, pp. 668–677 [accessed. 4. February 2014]. ISSN 1520-6106. Retrieved from: doi:10.1021/jp026731y

[11] VERELLEN, Niels, Yannick SONNEFRAUD, Heidar SOBHANI, Feng HAO, Victor V. MOSHCHALKOV, Pol Van DORPE, Peter NORDLANDER and Stefan A. MAIER. Fano Resonances in Individual Coherent Plasmonic Nanocavities. *Nano Letters* [online]. 2009, vol. 9, no. 4,

pp. 1663–1667 [accessed. 4. February 2014]. ISSN 1530-6984. Retrieved from: doi:10.1021/nl9001876

[12] LIU, Q., Y. CUI, D. GARDNER, X. LI, S. HE and II SMALYUKH. Self-alignment of plasmonic gold nanorods in reconfigurable anisotropic fluids for tunable bulk metamaterial applications. *Nano Lett* [online]. 2010, vol. 10, pp. 1347–53. ISSN 1530-6992 (Electronic) 1530-6984 (Linking). Retrieved from: doi:10.1021/nl9042104

[13] WANG, Libing, Yingyue ZHU, Liguang XU, Wei CHEN, Hua KUANG, Liqiang LIU, Ashish AGARWAL, Chuanlai XU and Nicholas A. KOTOV. Side-by-Side and End-to-End Gold Nanorod Assemblies for Environmental Toxin Sensing. *Angewandte Chemie International Edition* [online]. 2010, vol. 49, no. 32, pp. 5472–5475 [accessed. 4. February 2014]. ISSN 1521-3773. Retrieved from: doi:10.1002/anie.200907357

[14] SHARMA, Vivek, Kyoungweon PARK and Mohan SRINIVASARAO. Colloidal dispersion of gold nanorods: Historical background, optical properties, seed-mediated synthesis, shape separation and self-assembly. *Materials Science and Engineering: R: Reports* [online]. 2009, vol. 65, pp. 1–38. ISSN 0927796X. Retrieved from: doi:10.1016/j.mser.2009.02.002

[15] NIKOOBAKHT, B., Z. L. WANG and M. A. EL-SAYED. Self-assembly of gold nanorods. *Journal of Physical Chemistry B* [online]. 2000, vol. 104, pp. 8635–8640. ISSN 1089-5647. Retrieved from: doi:10.1021/Jp001287p

[16] MING, Tian, Xiaoshan KOU, Huanjun CHEN, Tao WANG, Hoi-Lam TAM, Kok-Wai CHEAH, Ji-Yao CHEN and Jianfang WANG. Ordered Gold Nanostructure Assemblies Formed By Droplet Evaporation. *Angewandte Chemie* [online]. 2008, vol. 120, no. 50, pp. 9831–9836 [accessed. 23. August 2013]. ISSN 1521-3757. Retrieved from: doi:10.1002/ange.200803642

[17] NOVOTNÝ, Filip, Jan PROŠKA, Ivan RICHTER and Pavel FIALA. Preparation of Metallo-Dielectric Diffractive and Plasmonic Structures via Self-Assembly. In: [online]. B.m.: Optical Society of America, 2009, p. AThA2. OSA Technical Digest (CD). Retrieved from: http://www.opticsinfobase.org/abstract.cfm?URI=AIOM-2009-AThA2

[18] NOVOTNÝ, Filip, Petr WANDROL, Jan PROŠKA and Miroslav ŠLOUF. In-Situ WetSTEM Observation of Gold Nanorod Self-Assembly Dynamics in a Drying Colloidal Droplet. *Microscopy and Microanalysis* [online]. 2014, vol. 20, no. 02, pp. 385–393. Retrieved from: doi:10.1017/S1431927614000208

[19] OZIN, Geoffrey. *Nanochemistry Reproducibility - MaterialsViews* [online]. 2014 [accessed. 24. September 2014]. Retrieved from: http://www.materialsviews.com/nanochemistry-reproducibility/

7 AUTHOR'S RELEVANT PUBLICATION ACTIVITIES

Impacted international journals:

- NOVOTNÝ, Filip, WANDROL, Petr, PROŠKA, Jan and ŠLOUF, Miroslav. In-Situ WetSTEM Observation of Gold Nanorod Self-Assembly Dynamics in a Drying Colloidal Droplet. *Microscopy and Microanalysis*. 2014. Vol. 20, no. 02, p. 385–393. DOI 10.1017/S1431927614000208.
- PHILIMONENKO, V. V., PHILIMONENKO, A. A., ŠLOUFOVÁ, I., HRUBÝ, M., NOVOTNÝ, F., HALBHUBER, Z., KRIVJANSKÁ, M., NEBESÁŘOVÁ, J., ŠLOUF, M. and HOZÁK, P. Simultaneous detection of multiple targets for ultrastructural immunocytochemistry. *Histochemistry and Cell Biology*. 1 March 2014. Vol. 141, no. 3, p. 229–239. DOI 10.1007/s00418-013-1178-6.

Articles in peer-reviewed conference proceedings:

- NOVOTNÝ, Filip a Jan PROŠKA. Image processing application in MathematicaTM: measuring complex shaped metal nanoparticles in noisy micrographs. In: International Microscopy Congress 2014: 18th International Microscopy Congress. Prague: Czechoslovak Microscopy Society, 2014.
- NOVOTNÝ, Filip, DĚDIČ, Jan and PROŠKA, Jan. Anisometric Gold Nanoparticle Self-Assembly At Water/Air Interface. In : *NANOCON 2013 - Conference Proceedings*. Brno, Czech Republic : TANGER spol. s.r.o., 17 October 2013.
- HAVEL, Filip, Filip NOVOTNÝ, Michal JELÍNEK, Jan PROŠKA, Kamil KUČA a Kamil MUSÍLEK. Optimalization of optothermal properties of gold nanorods. In: Nanocon 2013: NANOCON 2013 - Conference Proceedings. Brno, Czech Republic: TANGER spol. s.r.o., 2013.
- NOVOTNÝ, F., PROŠKA, Jan and PROCHÁZKA, M. CORRELATED RAMAN MICROSCOPE/SCANNING ELECTRON MICROSCOPE STUDY OF SELF-ASSEMBLED GOLD NANOROD ARRAYS. In : *NANOCON 2011 - Conference Proceedings*. Brno : TANGER spol. s r.o., 2011. p. P143. ISBN 978-80-87294-27-7.
- NOVOTNÝ, F. and PROŠKA, J. Surfactant Assisted Self-assembly of Seed Mediated Grown Gold Nanorods. In : *3rd EuCheMS Chemistry Congress* [online]. Frankfurt am Main : Gesellschaft Deutscher Chemiker e.V. (GDCh), 2010. p. la.59. Available from: http://va.gdch.de/wwwdata/abstracts/5576/5576_1536.pdf.
- NOVOTNÝ, F. and PROŠKA, J. A thermodynamic approach for interpretation of absorption spectra of gold nanorod colloidal solution. In : *2nd International Conference NANOCON 2010* [online]. Ostrava : TANGER, spol.s r.o, 2010. p. 25. ISBN 978-80-87294-19-2. Available from: http://www.nanocon.cz/data/nanocon2010/sbornik/lists/papers/569.pdf
- NOVOTNÝ, Filip, PROŠKA, Jan, RICHTER, Ivan and FIALA, Pavel. Preparation of Metallo-Dielectric Diffractive and Plasmonic Structures via Self-Assembly. In : [online]. Optical Society of America, 2009. p. AThA2. OSA Technical Digest (CD). Available from: http://www.opticsinfobase.org/abstract.cfm?URI=AIOM-2009-AThA2
- NOVOTNÝ, F., I. KRAKOVSKÝ, J. PLEŠTIL a J. PROŠKA. Preparation of Composite Nanomaterials Based On Metal Nanoparticles and Hydrogels. In: Nanocon 2009: Nanocon 2009 Conference Proceedings. Ostrava: TANGER, spol.s r.o, 2009, p. 88. ISBN 978-80-87294-13-0.

SUMMARY

The aim of the thesis was the shape-controlled synthesis of plasmonic nanoparticles, their self-assembly, and their biomedical applications. As a prototype for the entire field, gold nanorods (AuNRs) were chosen, for their anisotropic optical properties, and great tunability in the visible and near-infrared region of the electromagnetic spectrum. For better insight into the chosen method, seeded growth method in the presence of silver nitrate, extensive absorption kinetics study was conducted. It showed, that one must maintain good control of the excess of the reducing agent during synthesis to be able to fine-tune the dispersity and shape purity of the colloidal solution. Precise laboratory protocols for the synthesis of AuNRs suitable for biomedical applications were formulated. Two separate laboratory setups for the preparation of self-assembled AuNR arrays were presented. Self-assembly of AuNRs *in-situ* was directly observed using state-of-the-art environmental electron microscope. The interesting optical properties of AuNR arrays were explored through correlated electron microscope/optical microscope imaging. For the refinement of the AuNR colloidal sample characterization, software tools in Wolfram programming language based on *Mathematica*™ computational software were developed.

RESUMÉ

Cílem práce byla příprava plazmonických nanočástic, studium jejich samouspořádání a aplikace v biomedicíně. Konkrétní volba padla na zlaté nanotyčinky (AuNRs), které se nacházejí v centru zájmu oboru plazmoniky pro svůj výrazně anizometrický, protáhlý tvar a výbornou laditelnost optických vlastností ve viditelné a blízce infračervené části spektra. Pro hlubší vhled do vybrané metody přípravy, přerůstání zárodků v přítomnosti dusičnanu stříbrného, byla provedena rozsáhlá studie růstu AuNRs pomocí absorpčních kinetik. Ta ukázala, že pro dobrou kontrolu nad dispersitou koloidu a tvarovou čistotou nanočástic je je kritickým řídícím parametrem přebytek redukčního činidla v roztoku. Na základě tohoto studia byly zformulovány detailní laboratorní protokoly pro přípravu AuNRs vhodných pro biomecínské aplikace a teranostiku. Dále byly sestrojeny dvě laboratorní sestavy pro přípravu uspořádáných polí AuNRs. Samouspořádání AuNRs *in-situ* bylo pozorováno pomocí pokročilé environmentální elektronové mikroskopie. Netriviální optické vlastnosti uspořádaných polí AuNRs byly demonstrovány korelací elektronové mikroskopie a optické mikroskopie. Pro účely co nejpřesnější charakterizace koloidních roztoků AuNRs byly vytvořeny originální softwarové nástroje v programovém prostředí *Mathematica*™.